Journal of Low Temperature Physics manuscript No.
(will be inserted by the editor)

M. Yu. Kagan[1,2] · **V. A. Mitskan**[3,4] ·
M. M. Korovushkin[3]

Effect of the long-range Coulomb interaction on phase diagram of the Kohn-Luttinger superconducting state in idealized graphene

29.06.2015

Abstract The effect of the long-range Coulomb interaction on the realization of the Kohn-Luttinger superconductivity in idealized monolayer doped graphene is studied. It is shown that the allowance for the Kohn-Luttinger renormalizations up to the second order in perturbation theory in the on-site Hubbard interaction inclusively, as well as the intersite Coulomb interaction significantly affects the competition between the superconducting phases with the f-wave, $p+ip$-wave and $d+id$-wave symmetries of the order parameter. It is shown that the account for the Coulomb repulsion of electrons located at the next-nearest neighboring atoms in such a system changes qualitatively the phase diagram and enhances the critical superconducting temperature.

Keywords Unconventional superconductivity, Kohn-Luttinger mechanism, graphene monolayer

1 Introduction

At the present time, the possible development of superconductivity in the framework of the Kohn-Luttinger mechanism[1], suggesting the emergence of superconducting pairing in the systems with the purely repulsive interaction[2], in graphene under appropriate experimental conditions is widely discussed. Despite the fact that intrinsic superconductivity so far has not been observed in graphene, the stability of the Kohn-Luttinger superconducting phase has been investigated and the

[1]P. L. Kapitza Institute for Physical Problems, Russian Academy of Sciences,
Moscow 119334, Russia
[2]National Research University Higher School of Economics,
Moscow 109028, Russia
[3]L. V. Kirensky Institute of Physics, Siberian Branch of Russian Academy of Sciences,
Krasnoyarsk 660036, Russia
[4]M. F. Reshetnev Siberian State Aerospace University,
Krasnoyarsk 660014, Russia
E-mail: kagan@kapitza.ras.ru

arXiv:1511.00377v2 [cond-mat.supr-con] 1 Feb 2016

symmetry of the order parameter in the hexagonal lattice was identified. It was found[3] that chiral superconductivity[4] with the $d+id$-wave symmetry of the order parameter prevails in a large domain near the Van Hove singularity in the density of states (DOS). The competition between the superconducting phases with different symmetry types in the wide electron density range $1 < n \leq n_{VH}$, where n_{VH} is the Van Hove filling, in graphene monolayer was studied in papers[5,6]. It was demonstrated that at intermediate electron densities the Coulomb interaction of electrons located on the nearest carbon atoms facilitates implementation of superconductivity with the f-wave symmetry of the order parameter, while at approaching the Van Hove singularity, the superconducting $d+id$-wave pairing evolves[5,6].

In this paper, we investigate the role of the Coulomb repulsion of electrons located at the next-nearest neighboring carbon atoms in the development of the Kohn-Luttinger superconductivity in an idealized graphene monolayer disregarding the effect of the Van der Waals potential of the substrate and both magnetic and non-magnetic impurities. Using the Shubin-Vonsovsky (extended Hubbard) model in the Born weak-coupling approximation, we construct the phase diagram determining the boundaries of the superconducting regions with different types of the symmetry of the order parameter. It is shown that the account for the Coulomb repulsion of electrons located at the next-nearest neighboring sites of hexagonal lattice leads to a qualitative modification of the phase diagram, as well as an increase in the critical temperature of the transition to the superconducting state in the system.

2 Theoretical model

In the hexagonal lattice of graphene, each unit cell contains two carbon atoms. Therefore, the entire lattice can be divided into two sublattices A and B. In the Shubin-Vonsovsky model[7], the Hamiltonian for the graphene monolayer taking into account the electron hoppings between the nearest atoms, as well as the Coulomb repulsion between electrons located at one, neighboring and next-nearest neighboring atoms in the Wannier representation, has the form

$$\hat{H} = \hat{H}_0 + \hat{H}_{int}, \tag{1}$$

$$\hat{H}_0 = -\mu\left(\sum_{f\sigma}\hat{n}^A_{f\sigma} + \sum_{g\sigma}\hat{n}^B_{g\sigma}\right) - t_1\sum_{f\delta\sigma}(a^\dagger_{f\sigma}b_{f+\delta,\sigma} + \text{h.c.}),$$

$$\hat{H}_{int} = U\left(\sum_f \hat{n}^A_{f\uparrow}\hat{n}^A_{f\downarrow} + \sum_g \hat{n}^B_{g\uparrow}\hat{n}^B_{g\downarrow}\right) + V_1\sum_{f\delta\sigma\sigma'}\hat{n}^A_{f\sigma}\hat{n}^B_{f+\delta,\sigma'}$$
$$+ \frac{V_2}{2}\left(\sum_{\langle\langle fm\rangle\rangle\sigma\sigma'}\hat{n}^A_{f\sigma}\hat{n}^A_{m\sigma'} + \sum_{\langle\langle gr\rangle\rangle\sigma\sigma'}\hat{n}^B_{g\sigma}\hat{n}^B_{r\sigma'}\right).$$

Here, operators $a^\dagger_{f\sigma}(a_{f\sigma})$ create (annihilate) an electron with spin projection $\sigma = \pm 1/2$ at the site f of the sublattice A; $\hat{n}^A_{f\sigma} = a^\dagger_{f\sigma}a_{f\sigma}$ denotes the operator of the number of fermions at the f site of the sublattice A (analogous notation is used for the sublattice B). Vector δ connects the nearest atoms of the hexagonal lattice. We

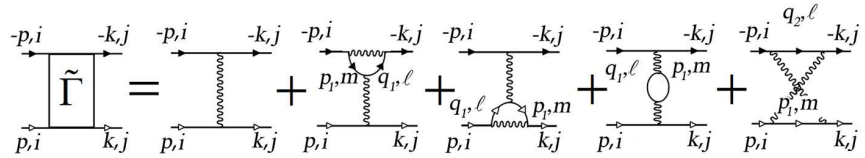

Fig. 1 The diagrams for the effective interaction of electrons in graphene monolayer. Solid lines with light (dark) arrows describe the Green functions for electrons with spin $+\frac{1}{2}$ $(-\frac{1}{2})$ and energies corresponding to the energy bands E_i and E_j (i and j are equal to 1 or 2). Here momenta $\mathbf{q}_1 = \mathbf{p}_1 + \mathbf{p} - \mathbf{k}$ and $\mathbf{q}_2 = \mathbf{p}_1 - \mathbf{p} - \mathbf{k}$ are introduced.

assume that the position of the chemical potential μ and the number of carriers n in graphene monolayer can be controlled by a gate electric field. In the Hamiltonian, t_1 is the hopping integral between the neighboring atoms (hoppings between different sublattices), U is the parameter of the Hubbard repulsion between electrons of the same atom with the opposite spin projections, and V_1 and V_2 are the Coulomb interactions between electrons of the neighboring and the next-nearest neighboring carbon atoms in the monolayer. In the Hamiltonian, the symbol $\langle\langle\ \rangle\rangle$ means that the summation is carried out only over the next-nearest neighbors.

Proceeding to the momentum space and performing the Bogoliubov transformation,

$$\alpha_{i\mathbf{k}\sigma} = w_{i1}(\mathbf{k})a_{\mathbf{k}\sigma} + w_{i2}(\mathbf{k})b_{\mathbf{k}\sigma}, \qquad i = 1,2, \tag{2}$$

we diagonalize Hamiltonian $\hat{H}_0$, which acquires the form

$$\hat{H}_0 = \sum_{i=1}^{2}\sum_{\mathbf{k}\sigma} E_{i\mathbf{k}}\alpha^{\dagger}_{i\mathbf{k}\sigma}\alpha_{i\mathbf{k}\sigma}. \tag{3}$$

The two-band energy spectrum is described by the expressions[8]

$$E_{1\mathbf{k}} = t_1|u_{\mathbf{k}}| - t_2 f_{\mathbf{k}}, \qquad E_{2\mathbf{k}} = -t_1|u_{\mathbf{k}}| - t_2 f_{\mathbf{k}}, \tag{4}$$

where the following notation has been introduced:

$$f_{\mathbf{k}} = 2\cos(\sqrt{3}k_y a) + 4\cos\left(\frac{\sqrt{3}}{2}k_y a\right)\cos\left(\frac{3}{2}k_x a\right),$$
$$u_{\mathbf{k}} = \sum_{\delta} e^{i\mathbf{k}\delta} = e^{-ik_x a} + 2e^{\frac{i}{2}k_x a}\cos\left(\frac{\sqrt{3}}{2}k_y a\right), \qquad |u_{\mathbf{k}}| = \sqrt{3 + f_{\mathbf{k}}}.$$

The utilization of the Born weak-coupling approximation with the hierarchy of model parameters

$$W > U > V_1 > V_2, \tag{5}$$

where W is the bandwidth in graphene monolayer (4), allows us to restrict the consideration only to the second-order diagrams in the calculation of the effective interaction of the electrons in the Cooper channel, and use the quantity $\widetilde{\Gamma}(\mathbf{p},\mathbf{k})$ for it. Note that this quantity is determined by the diagrams presented in Fig. 1.

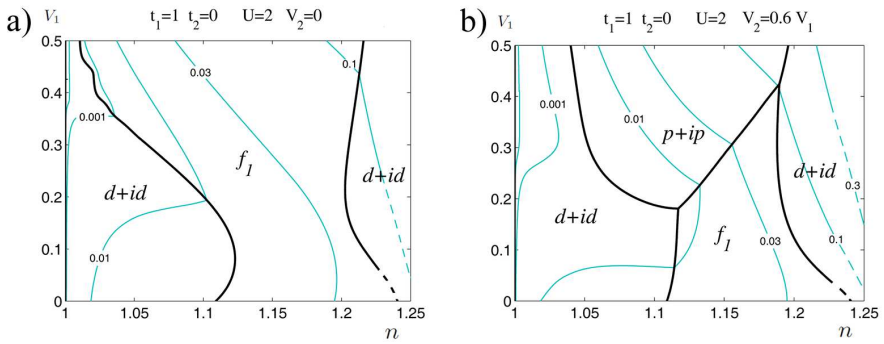

Fig. 2 (Color online) Superconducting phase diagram of an idealized graphene monolayer at $U = 2|t_1|$ for (a) $V_2 = 0$ and (b) $V_2 = 0.6V_1$. Thin blue lines show the lines of constant $|\lambda|$.

As far as the development of Cooper pairing is determined by the properties of the energy spectrum and the effective interactions of electrons in the vicinity of the Fermi level[9], we assume that the chemical potential of the system falls into the upper energy band $E_{1\mathbf{k}}$ and analyze the situation in which the initial and final momenta of electrons in the Cooper channel also belong to this band. In this paper, we perform the calculation of the superconducting phase diagram in graphene following to the scheme we used in our previous work[5].

3 Results

Figure 2a shows the calculated phase diagram of the superconducting state in graphene monolayer as a function of the carrier concentration n and V_1 for the set of parameters $U = 2|t_1|$ and $V_2 = 0$. It can be seen that the phase diagram consists of three regions. At low and high electron densities n, the chiral superconducting $d + id$-wave pairing is implemented[4,3]. At the intermediate densities, the triplet f-wave pairing occurs. With an increase of the intersite Coulomb interaction V_1, at low electron densities, the superconducting $d + id$-wave pairing is suppressed and the $f-$wave pairing is realized. In Fig. 2a, thin blue lines corresponding to the lines of constant absolute values of the effective coupling constant λ, show that in the vicinity of n_{VH} the values $|\lambda| = 0.1$.

In this paper, to avoid the consideration of the parquet diagrams[10,11], we analyze the electron concentrations for the regions which are not too close to the Van Hove singularity. In Fig. 2a, the dashed lines show the boundaries between the different regions of the superconducting pairing and the lines of $|\lambda|$ that are very close to n_{VH}.

Let us consider the influence of the Coulomb interaction V_2 between the electrons located at the next-nearest carbon atoms on the phase diagram for graphene monolayer. In Fig. 2b calculated for the fixed ratio between the parameters of the intersite Coulomb interactions $V_2 = 0.6V_1$, one can see that an account for V_2 leads to the qualitative modification of the phase diagram. This modification involves the suppression of the superconducting f-wave pairing at the large region

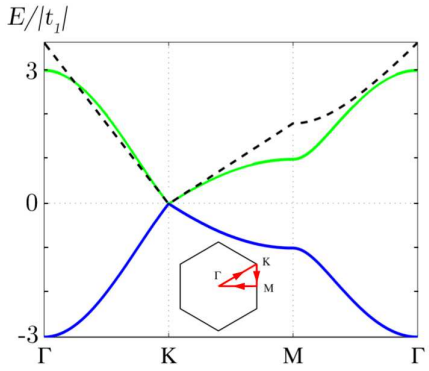

Fig. 3 (Color online) Energy spectrum of graphene monolayer defined by (4) (blue and green solid lines) and the spectrum obtained in the framework of the Dirac approximation (black dashed line). Subplot depicts the path around the Brillouin zone.

of intermediate electron densities and the realization of the chiral superconducting $p+ip$-wave pairing. Additionally, when V_2 is taken into account, the absolute values of the effective coupling constant increases to $|\lambda| = 0.3$. Consequently, it leads to a significant increase in critical temperatures of the superconducting transitions in idealized doped graphene. Note that here we do not analyze the account for the electron hoppings to the next-nearest carbon atoms t_2, because the consideration of these hoppings for graphene monolayer does not significantly modify the DOS in the carrier concentration regions between the Dirac point and both points n_{VH} [2,5].

Note that the Kohn-Luttinger superconducting pairing in graphene never develops in the vicinity of the Dirac points. Our calculations show that near these points, where the linear approximation for the energy spectrum of graphene works pretty well, the DOS is very low and the absolute values of the effective coupling constant $|\lambda| < 10^{-2}$. The higher values of $|\lambda|$, which can indicate the development of the Cooper instability at reasonable temperatures, arise at the electron concentrations $n > 1.15$. But at such concentrations, the energy spectrum of the monolayer along the direction KM of the Brillouin zone (Fig. 3) significantly differs from the Dirac approximation.

4 Conclusions

In conclusion, we have considered the conditions for the superconducting pairing in the framework of the Kohn-Luttinger mechanism in an idealized graphene monolayer, disregarding the influence of the Van der Waals potential, as well as structural disorder. The electronic structure of graphene is described in the Shubin-Vonsovsky model taking into account not only the Hubbard repulsion, but also the intersite Coulomb interactions. It is shown that the account of the Kohn-Luttinger renormalizations up to the second order of perturbation theory inclusively and the allowance for the Coulomb repulsion between electrons located at the neighboring

and the next-nearest neighboring carbon atoms determine to a considerable extent the competition between the f-, $p+ip$-, and $d+id$-wave superconducting phases. They also lead to a significant increase in the absolute values of the effective interaction and, hence, to the higher superconducting transition temperatures for the idealized graphene monolayer.

Note that for the p-, d-, f-wave, as well as for the s-wave pairing with nodal points in 2D ($\Delta_s(\phi) \sim \cos 6n\phi$, $\Delta_{s_{ext}}(\phi) \sim \sin 6n\phi$, $n \geq 1$), the Anderson theorem for non-magnetic impurities is violated and anomalous superconductivity is totally suppressed for $\gamma \sim T_c^{clean}$, where γ is an electron damping due to the impurity scattering ($\gamma = 1/(2\tau) = \pi n_{imp}|V_{el-imp}(0)|^2\rho_{2D}(\mu)$ in the Born approximation [12]).

Acknowledgements The authors thank V.V. Val'kov for stimulated discussions. The work is supported by the Russian Foundation for Basic Research (nos. 14-02-00058 and 14-02-31237). One of the authors (M. Yu. K.) thanks support from the Basic Research Program of the National Research University Higher School of Economics. The work of another one (M. M. K.) is supported by the scholarship SP-1361.2015.1 of the President of Russia and the Dynasty foundation.

References

1. W. Kohn, J. M. Luttinger, Phys. Rev. Lett. **15**, 524 (1965)
2. M. Yu. Kagan, V. V. Val'kov, V. A. Mitskan, M. M. Korovushkin, JETP **118**, 995 (2014)
3. R. Nandkishore, L. S. Levitov, A. V. Chubukov, Nature Phys. **8**, 158 (2012)
4. A. M. Black-Schaffer, C. Honerkamp, J. Phys.: Condens. Matter **26**, 423201 (2014)
5. M. Yu. Kagan, V. V. Val'kov, V. A. Mitskan, M. M. Korovushkin, Solid State Commun. **188**, 61 (2014)
6. R. Nandkishore, R. Thomale, A. V. Chubukov, Phys. Rev. B **89**, 144501 (2014)
7. S. Shubin, S. Vonsovsky, Proc. Roy. Soc. A **145**, 159 (1934)
8. P. R. Wallace, Phys. Rev. **71**, 622 (1947)
9. L. P. Gor'kov, T. K. Melik-Barkhudarov, JETP **13**, 1018 (1961)
10. I. E. Dzyaloshinskii, V. M. Yakovenko, JETP **67**, 844 (1988)
11. I. E. Dzyaloshinskii, I. M. Krichever, Ya. Khronek, JETP **67**, 1492 (1988)
12. A. I. Posazhennikova, M. V. Sadovskii, JETP Lett. **63**, 358 (1996)